Environmental Technology & Innovation 32 (2023) 103287

Contents lists available at ScienceDirect

Environmental Technology & Innovation

journal homepage: www.elsevier.com/locate/eti

Efficient treatment of bio-contaminated wastewater using plasma technology for its reuse in sustainable agriculture

Saeed Kooshki *, Pankaj Pareek, Robin Mentheour, Mário Janda, Zdenko Machala *

Faculty of Mathematics, Physics, and Informatics, Comenius University Bratislava, Slovakia

ARTICLE INFO

Article history:
Received 28 March 2023
Received in revised form 7 July 2023
Accepted 9 July 2023
Available online 13 July 2023

Keywords:
Plasma-activated water (PAW)
Plasma wastewater treatment
Fountain Dielectric Barrier Discharge (FDBD) reactor
Bactericidal effects
Seed germination enhancement
Wastewater treatment optimization

ABSTRACT

Water-related crisis represents one of the significant challenges of the rapidly growing world population. This study demonstrates an example of the novel technology of Non-Thermal Plasma (NTP) wastewater treatment for its sustainable recovery and reuse in agriculture. NTP treatment of wastewater not only causes microbial decontamination but produces Reactive Oxygen and Nitrogen Species (RONS), which can consequently improve seed germination and plant growth. We investigated the effects of the new Fountain Dielectric Barrier Discharge air plasma reactor for the treatment of bulk quantity water contaminated by *Staphylococcus epidermidis* or *Escherichia coli* bacteria. Then, employing the treated water for barley seed germination showed >20% enhancement compared to using tap water. The inactivation of bacteria in water was determined in dependence on pH, Oxidation-Reduction Potential, and correlated with chemical RONS produced in the water (hydrogen peroxide, nitrites, and especially nitrates). By utilizing the Responses Surface Methodology, we identified the optimal plasma treatment time per litre required for efficient RONS production and bactericidal effect in the wastewater treatment, which was linearly scalable with water volume. After the optimum plasma treatment time, a sharp drop in pH, and the concentrations of nitrites and hydrogen peroxide were observed, which is related to the peroxynitrite formation leading to the significant bacterial reduction up to 7-log.

1. Introduction

As the world population continues to grow at an alarming rate, several global challenges are emerging, among them being the water crisis. Climate change is causing water-related hazards such as droughts and floods that occur more frequently across the globe, while access to safe drinking water remains a critical issue in many countries. The World Health Organization recently reported that roughly two billion people use drinking water sources contaminated by faecal matter and microbial contamination, leading to around 485,000 fatalities annually (Anon, 2022). The 2018 edition of the United Nations World Water Development Report forecasts that almost six billion people will suffer from clean water scarcity by 2050. In the meantime, the global demand for water is expected to rise sharply in the next two decades, especially in agriculture, which accounts for the largest demand sector. The global demand for water for agricultural activities is predicted to increase by 60% by 2025 (Alberto and Lorenzo, 2019). To address these challenges, a lot of research is focusing on wastewater treatment as a resource to balance water demand across various sectors, including

* Corresponding authors.
E-mail addresses: Saeed.Kooshki@fmph.uniba.sk (S. Kooshki), machala@fmph.uniba.sk (Z. Machala).

https://doi.org/10.1016/j.eti.2023.103287

agriculture. However, conventional wastewater treatment methods have several disadvantages, such as non-reactive chemical residues, low efficiency against some organic and biological pollutants, high running costs, and the emission of pollutants such as dioxins into the environment (Gururani et al., 2021). To overcome these limitations of conventional wastewater treatment methods, great scientific efforts are being put into the establishment of advanced oxidation processes for treating wastewater and microbial inactivation, such as photo-Fenton techniques, photocatalysis, ozonation, electrochemical reactions, irradiation technology, and non-thermal plasma technology, or their combinations (Barjasteh et al., 2021; Ameta and Ameta, 2018).

Non-thermal plasma (NTP) technology is emerging as a sustainable solution to address some of these challenges. Plasma, which is the fourth state of matter, is a mixture of positive and negative ions, electrons, photons, and neutral particles. NTP (also referred to as cold plasma) is distinguished from thermal plasma by having much higher electron energy than that of ions and neutral particles, while keeping the overall gas temperature close to room temperature. Adamovich et al. outlined NTP science as a sustainable technology that has made a significant impact on various applications in industry and society such as plasma medicine, plasma pollutant control, plasma agriculture and innovative food cycles (Bogaerts et al., 2020; Puač et al., 2018). It should be highlighted that the most impactful current NTP applications in industry have no alternative (Adamovich et al., 2022).

Plasma-Activated Water (PAW) can be generated through direct or indirect NTP interactions with water. The treatment or application of cold plasma above or inside water initiates many reactions in surrounding environment above and inside water without the involvement of added chemicals. Compared to Advanced Oxidation Processes (AOP), PAW technology offers some advantages for wastewater treatment, including the ability to control various physical, chemical, and biological parameters of water such as pH, salinity (Ekanayake et al., 2021), conductivity, Oxidation-Reduction Potential (ORP), turbidity, hardness (Aka et al., 2022), chemical contaminants (Magureanu et al., 2015; Wardenier et al., 2019), and microbial load (Patinglag et al., 2021). Additionally, cold plasma treatment enriches water with produced Reactive Oxygen and Nitrogen Species (RONS). The RONS in PAW usually include long-lived species, such as nitrates (NO_3^-), nitrites (NO_2^-), and hydrogen peroxide (H_2O_2), with corresponding typical half-lifetimes of years, days, and hours, respectively, and short-lived ones such as hydroxyl radicals ($OH^\bullet$), nitric oxide ($NO^\bullet$), superoxide (O_2^-), peroxynitrate ($OONO_2^-$), and peroxynitrite ($ONOO^-$) with sub-second lifetimes (Thirumdas et al., 2018; Zhou et al., 2018). These plasma-generated reactive chemical species transported in PAW play a crucial role in different biological applications of PAW such as: cancer cell treatment (Harley et al., 2020), dentistry (Milhan et al., 2022), wound healing (Xu et al., 2020b), disinfecting the spoilage microorganisms and foodborne pathogens on food products for the reduction of post-harvest losses, and production of safer foods, as well as to replace the traditional chemical sanitizing solutions applied for disinfection (Thirumdas et al., 2018; Herianto et al., 2023). Mixture of various plasma-generated reactive oxygen species (ROS) including singlet molecular oxygen $^1O_2$, in bio-contaminants inactivation during wastewater disinfection have been demonstrated to have better antimicrobial ability than a mimicked solution of single ROS (Xu et al., 2022).

Moreover, the RONS in PAW have been demonstrated to have significant beneficiary effects in agriculture applications. PAW operates as a green fertilizer better than synthetic chemical fertilizer (Zhang et al., 2017). The plasma-induced RONS might be utilized to enhance seed germination (Šerá et al., 2021), seedling growth (Ndiffo Yemeli et al., 2021), promote plant growth (Rathore et al., 2022), maintain the quality of postharvest (Xu et al., 2016), preservation of fruits and vegetables (Soni et al., 2021), and controlling plant diseases and pests (Bertaccini et al., 2017). The use of PAW technology has the potential to significantly contribute to reducing global warming, since currently, the fertilizer production accounts for approximately 1.2% of the global energy consumption (Ghavam et al., 2021), and the use of fossil fuels as the primary feedstock for traditional Haber-Bosch ammonia production results in about 1.4% of global carbon dioxide emissions annually (MacFarlane et al., 2020). PAW technology also offers an alternative to traditional fertilizer production: the reactive nitrogen species present in PAW can serve as a green liquid fertilizer for seed germination and plant growth. Gao et al. have suggested in a recent comprehensive review that PAW technology can be used as a sustainable and sanitation method for the water system (Gao et al., 2022a). In fact, using PAW technology for wastewater treatment can catch four birds with one stone: (1) treatment of chemical water pollutants, (2) treatment of biological water contaminations, (3) producing nitrogen fertilizer without using chemical agents in water, and (4) by using local renewable electricity, it also avoids CO_2 emissions. Therefore, PAW technology development represents a huge potential for the total environment protection.

Despite its simplicity, eco-friendliness, economy, and ease of use in various physical conditions, such as ambient temperature and pressure, PAW technology still faces technological challenges in terms of process optimization and scale-up (Adamovich et al., 2022). The efficiency of plasma-chemical activation of large volumes of water is hindered by the limited transfer of gaseous reactive species to water (Gao et al., 2022b). Various plasma setups have been reported for PAW generation, such as corona discharge (Grabowski et al., 2007), gliding arc discharge (Terebun et al., 2021), transient spark (Machala et al., 2013), microwave plasmas (Qian et al., 2020), plasma jets, and Dielectric Barrier Discharges (DBD) (Judée et al., 2018). Hybrid plasma discharge, produced by two simultaneous plasma discharges, has been reported to improve energy efficiency (Hadinoto et al., 2023), but the total RONS concentrations were insufficient for high bacterial inactivation in the high-volume (more than 2 litre) PAW generation. Bubble-enhanced cold plasma activation is another method that can enhance energy efficiency in plasma activation. Gao et al. reported a bubble-plasma system using a plasma jet and venturi tube, but for a bulk quantity of water the RONS concentrations just reached a few ppm (Gao et al., 2022b).

In this study, we utilized a novel DBD reactor with the capability to process relatively large wastewater volumes. To simulate bio-contaminated wastewater, we contaminated regular tap water with Gram-negative bacteria *Escherichia coli* or Gram-positive bacteria *Staphylococcus epidermidis*. *E. coli* is a strong indicator of sewage or animal waste pollution in water, potentially harbouring numerous disease-causing organisms and present in untreated water and food. *S. epidermidis*, mainly linked to human skin and mucous membranes, primarily contaminates wastewater through human-related activities, including the introduction of materials originating from humans into wastewater systems via various channels like domestic, hospital, healthcare, and industrial wastewater. Because of the antibiotic resistance genes and the ability to form biofilms, *S. epidermidis* bacteria contamination is more difficult to treat (Siciliano et al., 2023), therefore in this study, we prioritize the treatment of wastewater contaminated by *S. epidermidis* bacteria. Therefore, all the bacteria reduction data are referred to *S. epidermidis* unless specified for *E. coli* in the results section. The contaminated water was treated with the DBD reactor to remove contaminants and transfer RONS into the water for PAW production. We then compared the germination rate of barley seeds soaked in the plasma-treated contaminated water to those soaked in fresh water. We utilized Response Surface Methodology (RSM) to determine the optimum plasma treatment time for the maximum RONS production and bacteria reduction by varying the experimental conditions.

2. Materials and methods

2.1. Plasma-activated water setup

A Fountain Dielectric Barrier Discharge (FDBD) reactor was designed to treat bulk quantity of water at relatively high flow rates (up to 2.3 l min^{-1}). The flowing pattern of water in the FDBD reactor resembles a fountain. Water is pumped upward and then falls from the top of the central electrode tube laminarly on its outer circumference and passes through the microdischarge area. Fig. 1 shows the FDBD reactor with the liquid flowing in the direction of arrows. The PAW setup includes the FDBD reactor, water pump, water tank, high voltage AC transformer (15 kV, 20 kHz), variable autotransformer (variac), and DC power supply (24 V DC) for the water pump. The FDBD reactor has a coaxial cylindrical shape. A (200 $\times$ 30 mm) quartz tube with 1.5 mm thickness was used between the electrodes as the dielectric and the gap distance was around 4 mm. The inner electrode was a copper tube with 170 $\times$ 22 mm dimensions. Aluminium foil used as the external electrode covered the quartz tube in the length around 13 cm.

The FDBD reactor design has some similarities with the falling film DBD reactor used by Kovacevic et al. but is different from several points of view. In the falling film DBD reactor (Kovačević et al., 2017), the inner tube features double walls that entirely separate the inner grounded electrode from the liquid. The falling film DBD reactor comprises a Pyrex tube with a double dielectric barrier between the electrodes, while the FDBD reactor has a single dielectric and lacks a grounded electrode. Moreover, a peristaltic pump is employed in a batch process in the falling film reactor, with distilled water being pumped at a constant flow rate, and the liquid is accumulated and transferred into the reactor again for longer plasma treatment time. Conversely, our FDBD reactor has a continuous circulation system with variable flow rates of wastewater and is a closed system without any gas injection, unlike the falling film DBD reactor, which features a gas injecting system. The closed system of the FDBD reactor, which does not have gas injection or exhaust, allows both plasma gas and water to exit through a single line, which enhances the chances of interaction during the entire process. Due to these differences, the FDBD reactor exhibits a higher yield of RONS formation in less plasma treatment time and consumes less power than the falling film DBD reactor.

In our FDBD reactor, water flows in the central tube electrode upward vertically and falls dawn on the outer surface of the electrode, where it interacts with the DBD plasma. The large diameter of the central electrode not only provides a vast range of variation for water circulation flow rate in the reactor, but also laminar flow through the gap distance. The water flow rate during circulation in the reactor varied from 0.9 to 2.3 l min^{-1} as a main process parameter in the experiments. The variac attached to the AC high voltage neon transformer allows us to smoothly change the applied input voltage and the discharge power. The input voltage as a main parameter in the PAW generation was varied between 120–220 V in 5 levels. The duration of interaction between plasma and recirculating water defined as the plasma treatment time, which is another main parameter in our experiments. Statistical analysis of the main parameters was carried out using the Responses Surface Methodology (RSM) in the central composite Design of Experiment (DOE) by the Minitab 19 program software.

2.2. Physical characterization of the plasma

Measurement of the plasma gas temperature and diagnostics of the reactive species generated in the plasma zone were performed using Optical Emission Spectroscopy (OES). Compact emission spectrometer Avantes AvaSpec-Mini4096CL (wavelength range 200–1100 nm, spectral resolution 0.5–0.7 nm) was used to collect the plasma emissions from the top of the FDBD reactor.

From the economical point of view, the total power consumption of the system is important. The total power consumption of the FDBD reactor was measured using a power meter Metex 3860M directly from the plug during the experiments. The voltage amplitude applied to the electrodes at different input voltages was measured using an oscilloscope and two high voltage probes with an attenuation ratio 1:1000. We used one high-voltage probe to measure

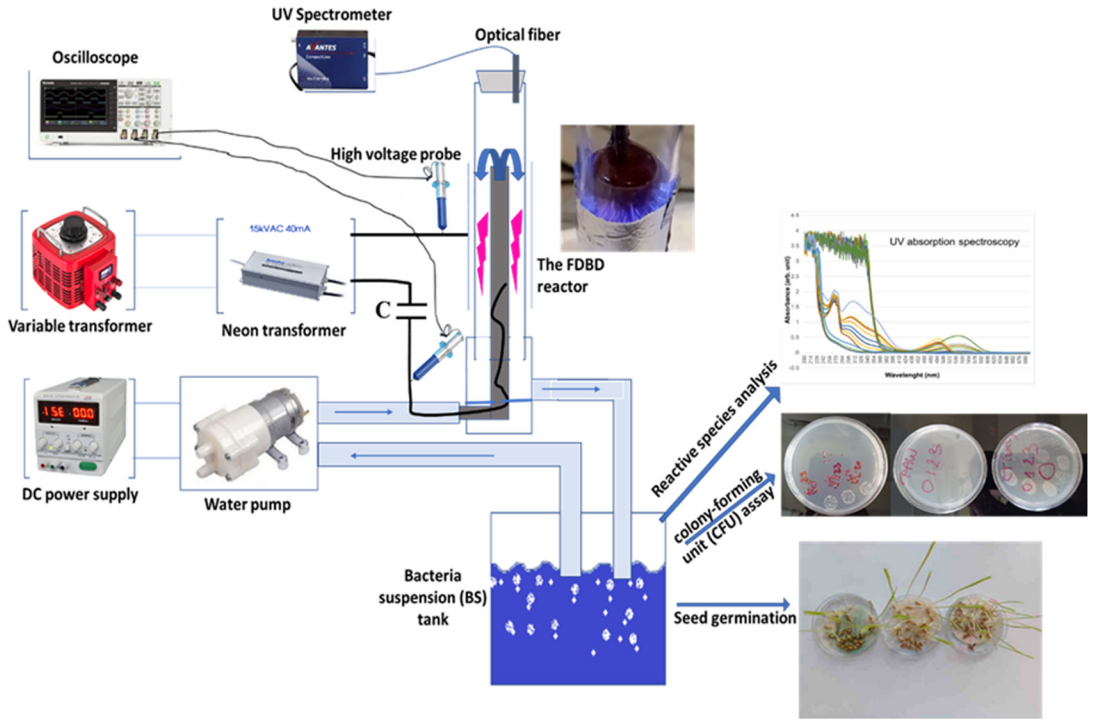

Fig. 1. Schematic overview of the experimental set up.

the voltage between the electrodes and another high voltage probe to measure the applied voltage on the equivalent capacitor (V_c) in the FDBD reactor. Various Lissajous figures were recorded by the oscilloscope Tektronix TBS2000 series, when the supplied voltage signals from both high voltage probes were driven into X-Y representation of two oscilloscope channels, to determine the power consumption by the plasma discharge. The area inside the closed Lissajous curve corresponds to the energy dissipated by the discharge per period. The transported charges in the discharge are determined indirectly through a 560 pF circuit equivalent capacitor, C_e. The voltage across C_e is proportional to the transported charge in the discharge, while the applied voltage is adequately high to cause breakdown in the gap. Thus, the average power dissipated in the discharge per cycle, P, can be calculated as follows:

$$P = \frac{1}{T}\int_0^T V.Idt = f\int_0^T V.C_e.\frac{dV_c}{dt}dt = f.\oint V.dq_c = f.S \tag{1}$$

Where f and S are the frequency applied and the area of Lissajous figure, respectively.

2.3. PAW effects on bacteria and seeds

Bacteria Suspension (BS) (i.e. bacteria contaminated water) for each experiment was prepared by mixing one litre of tap water with 10 ml of the bacteria sample. Bacteria sample of Gram-positive *Staphylococcus epidermidis* (ATCC 35984) or Gram-negative *E. Coli* (CCM 3954) was suspended in water in the planktonic form with an initial population of about 10^8 colony forming units per ml (CFU ml^{-1}). The procedure of preparing samples for both bacteria was the same. The bacteria samples were prepared by the dissolution of bacteria cultivated on sterile liquid nutrient (Lauria–Bertani broth, Biolab). After overnight cultivation (∼18 h at 37 °C) bacteria were active and vital in the stationary phase. The bacterial samples were diluted 1:10 in tap water to prepare BS then treated by the FDBD reactor at different plasma treatment time following the DOE conditions. The number of bacteria cells in the suspension was evaluated immediately after plasma treatment by counting CFUs cultivated on agar plates (Lauria–Bertani agar, Biolab) for 16–18 *h* at 37 °C. Just after the experiment, bacteria were diluted several times into deionized water to stop the plasma agents' activity. They were then spread on agar plates in Petri dishes and incubated overnight. The standard CFU cultivation method was employed. Values of 1, 2, 3 decadic log reduction of bacteria population correspond to the inactivation of 90%, 99%, 99.9% of the bacteria, respectively. Bacterial experiments were conducted in 4 repetitions.

Besides its antibacterial properties, the produced PAW can also be used as a fertilizer. Barley seeds were used as model seeds to investigate the effects of PAW on germination. *In vitro* cultivation of the seeds was performed on filter paper in Petri dishes. Four Petri dishes per variant were cultivated. The seed cultivation was performed in the laboratory condition

Table 1
Electrical characterizations of the FDBD reactor versus different input voltages.

Input voltage (V)	f (kHz) ± 0.1	Voltage amplitude (kV) ± 0.1	V_{pp} (kV) ± 0.1	Area of Lissajous figures (mCV)	Plasma power consumption (W)	Total power consumption (W)
120	18.7	6.7	13.0	2.7 ± 0.3	51 ± 6	130 ± 2
140	18.9	6.9	13.75	3.2 ± 0.4	60 ± 8	150 ± 2
170	19.2	7.1	14	3.7 ± 0.3	71 ± 6	190 ± 4
200	19.4	7.3	14.5	4.6 ± 0.4	89 ± 8	230 ± 5
220	19.5	7.4	14.75	5.2 ± 0.4	100 ± 8	270 ± 5

(dark chamber at temperature 22 ± 1 °C, 4 days). Samples of 30 seeds were placed in Petri dishes containing two layers of filter paper below and on the seeds. The seeds were soaked using 4 ml of the obtained PAW (prepared from BS) for each Petri dish. The number of germinated seeds was observed and recorded every day until the fourth day. The germination percentages of barley seeds were measured and compared with control samples provided from using normal tap water or bacteria contaminated water (BS). The emergence of radicles elongated more than 2 mm from the seed coat was taken as the criteria for germination. Germination percentage of barley seeds were calculated as following:

$$\text{Germination rate } (\%) = \frac{N_1}{N_0} \times 100\% \tag{2}$$

Where N_0 is the total number of seeds in each group and N_1 is the number of germinated seeds.

2.4. Chemical analysis of PAW

pH, Oxidation-Reduction Potential (ORP) and temperature were monitored for each plasma treated BS sample using a portable pH/ORP meter (WTW 3110, Weilheim, Germany). Electrical Conductivity (EC) of PAW samples was measured by Digital Conductivity Meter GMH 3430.

H_2O_2 concentration was measured by titanium oxy-sulfate ($TiOSO_4$) assay in acidic conditions (4 g l^{-1} $TiOSO_4$ 1:1 with concentrated H_2SO_4) (Lukes et al., 2014). H_2O_2 and Ti^{4+} reacts to form per-titanic acid H_2TiO_4, which is a yellow-coloured complex having absorption maximum at 407 nm. To prevent the decomposition of H_2O_2 by NO_2^- in acidic conditions, the PAW samples were stabilized by sodium azide NaN_3 (60 mM) immediately after the plasma treatment experiments. The volume ratio for the measurement of H_2O_2 concentration were NaN_3: sample: $TiOSO_4$ reagent = 1:10:5.

NO_2^- and NO_3^- concentrations were obtained by using Griess reagents in acidic conditions. Nitrites (NO_2^-) react with Griess reagents to form a purple azo compound with the absorption maximum at 540 nm (Machala et al., 2013).

Concentration of NO_3^- was evaluated by subtracting NO_2^- concentration from the total NO_x^- concentration. The total NO_x^- concentration was evaluated by using 10 mM 2,6-xylenol and acid (H_2SO_4:H_3PO_4 as 1:1) mixture as the reagent. The 10 mM xylenol mixture was prepared by adding 122.16 mg of 2,6-xylenol to 100 ml of 10% glacial acetic acid. The used volume ratio of sample: acid:xylenol was 1:8:1. The absorption maximum was recorded between 290 nm and 350 nm. A control sample was prepared with de-ionized water with the same procedure. The absorption maximum was recorded between 290 nm and 350 nm after subtracting the control in this region. The maximum peak is directly proportional to the concentration of NO_x^-. Finally, NO_3^- concentration was obtained by subtracting NO_2^- concentration from NO_x^- concentration (Veronico et al., 2021; Moorcroft et al., 2001).

3. Results and discussion

3.1. Plasma characterization

The primary external control parameter for generating the plasma discharge is the applied voltage. Typical electrical parameters, such as voltage and current waveforms, and Lissajous figures for discharge power measurement at different input voltages are plotted in Fig. 2. The applied frequency (f), maximum peak-to-peak value (V_{PP}), and the amplitude of the sinusoidal voltage given by the power supply in the experiments were varied in the range (18–20) kHz, (13–15) kV, and (6–8) kV by the variac at different input voltages, respectively. The sinusoidal voltage and current are shown in Fig. 2(a).

As shown in Fig. 2(b), the area of Lissajous curve was slightly increased with the increase in the input voltage applied to the FDBD reactor. Table 1 shows the total power consumption, plasma power consumption, and characterization of the applied voltage and frequency on the electrodes at different input voltages in the FDBD reactor. The total power consumption of the system includes plasma power consumption, water pump consumption, and heat losses of the system.

The main heat loss mechanism in the system is related to the dissipated power in the water. The water temperature timeline was recorded for the total volume of 1 l and 3 l water treatment (Fig. 3) using the FDBD. In the process of producing PAW, around 40% of energy is consumed as the plasma discharge power, and approximately 26%, 29%, and

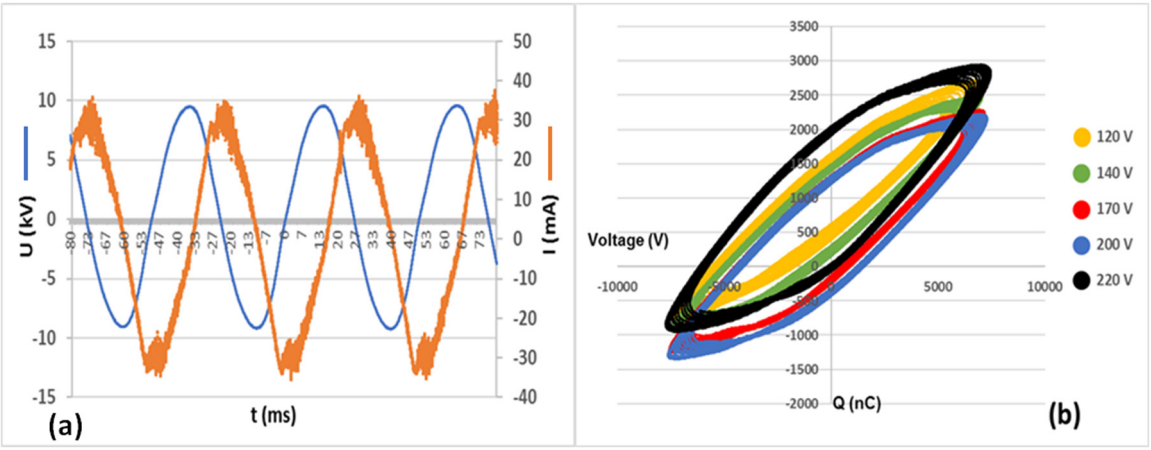

Fig. 2. (a) Voltage-current waveforms at the 220 V input voltage, (b) Lissajous curves at the different input voltages with electrode gap distance 4 mm (the water flow rate was held at 1750 ml min^{-1}).

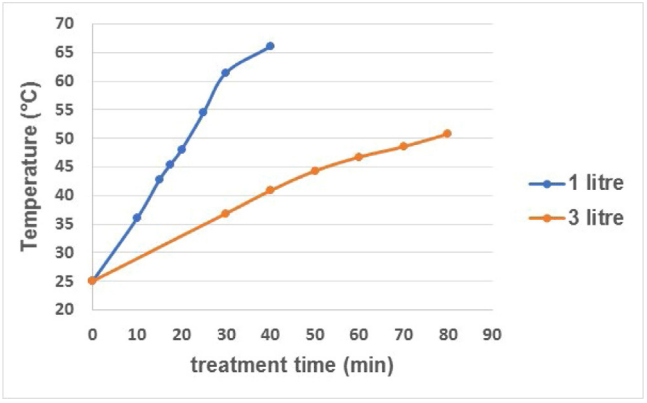

Fig. 3. Temperature timeline for 1 l and 3 l volume of plasma treated water by the FDBD reactor.

5% are dissipated as the water heating, reactor heating, and the water pump consumption, respectively. For example, for producing 1 l PAW with 20 min treatment time, the total consumed energy is around 342 kJ, from which around 137 kJ is related to plasma discharge energy, and 89 kJ is lost as water heating.

The identification various emissive reactive species and radicals present in air DBD plasma with water was performed by analysing their emission spectra, as shown in Fig. 4. As typical with atmospheric air NTP, N_2 emission spectra were dominant. Fig. 4(a) shows a high intensity emission of N_2 second positive system (SPS), corresponding to transition from excitation level $C^3\Pi_u$ to $B^3\Pi_g$, along with a very weak intensity OH ($A^2\Sigma^+ - X^2\Pi_{3/2}$) emission system. OH radicals were formed typically from water vapour present in the air plasma, and play crucial roles in bactericidal effects of the produced PAW. The presence of N_2 SPS emission indicate the presence of energetic electrons that initiate ionizations in the FDBD reactor, because the excitation energy threshold for level $C^3\Pi_u$ is above 11 eV. Thus, excited N_2 have enough energy to dissociate O_2 molecules resulting in the generation of atomic O, hence subsequent formation of O_3, NO and NO_2.

Experimental spectra of N_2 SPS emitted in air discharge are used for plasma temperature evaluation, since they enable to determine rotational T_r and vibrational T_v temperatures by fitting them with the simulated spectra. We used Specair software for spectral simulation (Laux, 2002). One of the best experimental spectra fit with the simulated ones is shown in Fig. 4(b) with $T_r = 700$ K. Considering fast collisional relaxation at atmospheric pressure, the gas temperature T_g equals with T_r. Vibrational temperature, $T_v \gg T_r$, indicates the non-equilibrium plasma conditions. It was measured by multiple N_2 SPS bands as shown on Fig. 4(c). Although, the vibrational temperature may not be well defined since vibrational states do not follow the Boltzmann distribution in strongly non-equilibrium conditions (Machala et al., 2007). Finally, N_2 first positive system ($B^3\Pi_g - A^1\Sigma_u^+$) and a weak emission of atomic N and O radicals as can be observed in the Vis-NIR spectral region in Fig. 4(d).

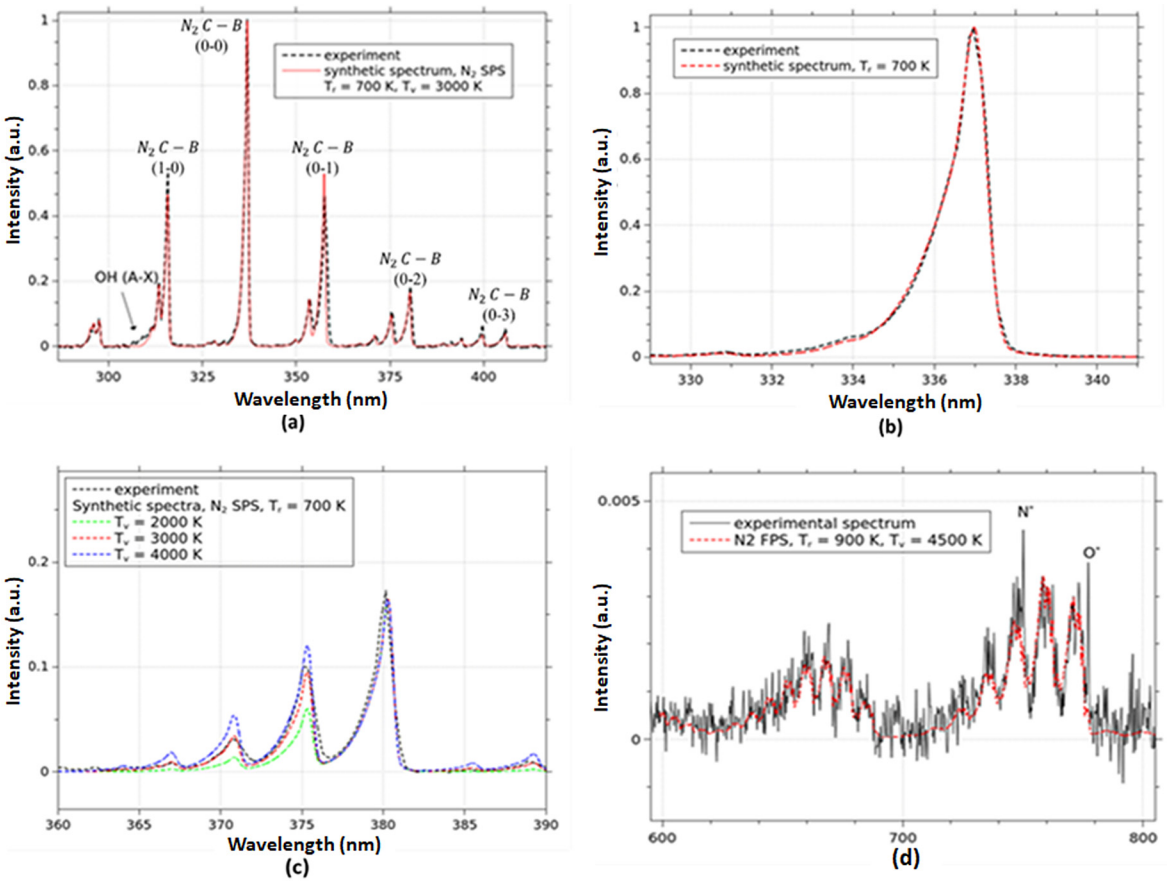

Fig. 4. Typical emission spectra of the FDBD reactor in UV region (corrected for the spectrometer's spectral response). Gap: 4 mm; f: 19.4 kHz; input voltage: 220 V. (a) N_2 second positive system (SPS) spectrum, (b) a high intensity emission of N_2 SPS 0–0 vibrational band fitted with the simulated spectrum, (c) multiple N_2 SPS bands fitted to estimate vibrational temperature, and (d) emission of N_2 first positive system and atomic *N* and O lines.

3.2. RONS and physicochemical properties of PAW

The experimental conditions according to the Design of Experiment (DOE) with subsequent responses are listed in Table 2. The initial value of pH, ORP and EC for tap water and bacteria contaminated water are mentioned in Table 2 as well. Then, using Responses Surface Methodology (RSM) the optimum parameter area for each response was determined.

Contour plots for different responses using the RSM analysis were studied to find out the optimum parameter area of the plasma treatment time, plasma input voltage and water circulation flow rate in the FDBD reactor as the main parameters of the experiments. From the economical point of view, plasma treatment time is the main parameter which must be minimized because it plays the main role in the total electrical power consumption for PAW generation by the FDBD reactor. However, some of the responses do not show any optimum area. For example, increasing the plasma treatment time and the power cause monotonous decrease of pH, and increase ORP and EC, which is confirmed by previous reports on other typical PAW properties (Canal et al., 2019; Machala et al., 2013).

Fig. 5 shows the contour plots of the produced long-lived RONS concentrations obtained in the PAW samples. The maximum concentration of H_2O_2 ($\approx$7 mg l^{-1}) was achieved in around 20 min plasma treatment time while the input voltage was held on the maximum value 220 V (Fig. 5(a)). In Fig. 5(b) concentrations of nitrites have practically the same behaviour as H_2O_2 concentration versus plasma treatment time and input voltage. Both NO_2^- and H_2O_2 concentrations reached their maximum levels at a certain plasma treatment time with maximum input voltage, and after that their concentrations decreased for longer treatment times. These rise and fall pattern behaviours are due to the mutual reaction between nitrites and H_2O_2 which leads to their decay under acidic conditions and proceeds to the formation of peroxynitrous acid (O = NOOH) or its conjugate base peroxynitrite anion ($O = NOO^-$) (Machala et al., 2013) summarized as:

$$NO_2^- + H_2O_2 + H^+ \rightarrow O = NOOH + H_2O \quad (3)$$

Table 2
Design of experiments according to the central composite of DOE.

Run order	Treatment time (min)	Flow rate (l min^{-1})	Input voltage (V)	pH ± 0.1	ORP ± 0.5 (mV)	EC ± 5 (μS/cm)
1	10	2.1	200	7.06	6	674
2	20	1.75	120	7.28	−5.7	709
3	30	2.1	200	3.1	223	950
4	20	1.75	170	7.15	1	693
5	37	1.75	170	3.68	191.2	823
6	20	1.75	170	6.88	16.2	706
7	10	2.1	140	7.25	−4	661
8	10	1.3	200	7.19	−1	641
9	20	1.75	170	6.96	11.8	693
10	20	2.5	170	6.76	22.4	728
11	10	1.3	140	7.41	−12.4	665
12	30	2.1	140	6.47	39.1	716
13	30	1.3	140	6.14	57	715
14	20	1.75	220	3.91	178.8	773
15	3	1.75	170	7.42	−13.4	654
16	20	0.9	170	6.86	16.9	700
17	30	1.3	200	3.03	226.9	955
18	20	1.75	170	6.96	11.9	690
19	20	1.75	170	7.01	7	687
20	20	1.75	170	6.92	13.9	682
Tap Water (TW) control				7.77	−32.7	425
Bacteria Suspension (BS) control				7.70	−29.0	630

For NO_2^- only, there is another maximum at treatment time >35 min at input voltage of 180 V, which must be related to enhanced gaseous NO_x and HNO_x formation as the temperature increases for longer treatment times, and correlates with NO_3^- plot (Fig. 5(c)). Also, higher temperature accelerates the reaction (3), leading to a stronger depletion of H_2O_2 while NO_2^- are in excess. Peroxynitrites are strong oxidants with an intense bactericidal effect, and they may significantly contribute to the bacteria inactivation process induced by air plasma in water. Measurement of temporal evolution of H_2O_2 and NO_2^- concentrations in plasma treated water showed that they progressively decreased with plasma treatment time (Fig. 5(a) and (b)), supporting the involvement of H_2O_2 in the decay of NO_2^- via peroxynitrite mechanism. $ONOO^-$ subsequently decay into the final product nitrates NO_3^-. This is supported by the results shown in Fig. 5(c) that demonstrate a significant increase in the concentrations of NO_3^- after 20 min plasma treatment time, which confirms the expected pH-dependent reaction between nitrites and H_2O_2 taking place in the PAW. NO_3^- are also additionally formed by direct NO_2^- disproportionation in acidic conditions without involvement of H_2O_2 (Lukes et al., 2014). The formation of NO_2^- and NO_3^- in the PAW due to dissolution of plasma-formed gaseous NO_x and HNO_x in water leads to the decrease of pH, as shown in Fig. 5(d). The evaluation of pH contour plot shows that it slightly decreases from the initial value of 7.7 to 5 before 20 min plasma treatment time, and then it suddenly falls below 3–4 after this critical point. All these contour plots indicate that the optimum area of the main parameters of PAW generation per 1 litre treated water using the FDBD reactor can be expected in the plasma treatment time and input voltage around 20 min and 220 V, respectively.

In addition, there is an optimum point in water flow rate parameter to achieve the maximum RONS concentrations (≈1750 ml min^{-1}) which is shown in Fig. 5(e) and (f). Any change in water flow rate can result in variation of the water layer thickness on the central electrode and it may subsequently change the gap distance and excitation energy of the plasma in the FDBD reactor. The following results were obtained with a fixed 1750 ml min^{-1} water flow rate to find more about plasma treatment time effects.

3.3. Antibacterial effects and germination enhancement

Inactivation efficiency of bacteria suspended in the water treated directly by the FDBD plasma reactor correlates with the RONS generation in the liquid. The disinfection efficiency against bacteria is mainly attributed to the oxidative stress induced by reactive oxygen species in PAW. Fig. 6 shows the EC and ORP contour plots (Fig. 6(a) and (b)) which have very similar behaviours with the bactericidal efficacy contour plot (Fig. 6(c)). It is generally established that the integrity of cell membrane, as well as the cell internal components and structure can be damaged by the oxidative stress induced by PAW (Xu et al., 2021; Zhang et al., 2013).

Our results show that the bactericidal effect of PAW increased with the plasma treatment time and input voltage. The bactericidal effect of PAW has a similar trend with the NO_3^-, pH, EC and ORP contour plots (Figs. 5(b), (c) and 6(a), (b), (c)). The NTP inactivation process exhibits a synergistic antimicrobial effect with RONS in the presence of acidic pH. These results agree with previous reports that the acidic environment combined with plasma agents, with a special role of the mutual reaction of H_2O_2 and nitrites (Eq. (3)) leading to ONOOH, hence to OH and NO_2^- radicals, lead to the bacterial inactivation (Machala et al., 2013, 2018; Zhang et al., 2016). The cell membrane peroxidation by RONS is probably the primary mechanism in plasma bio-decontamination (Machala et al., 2013, 2018).

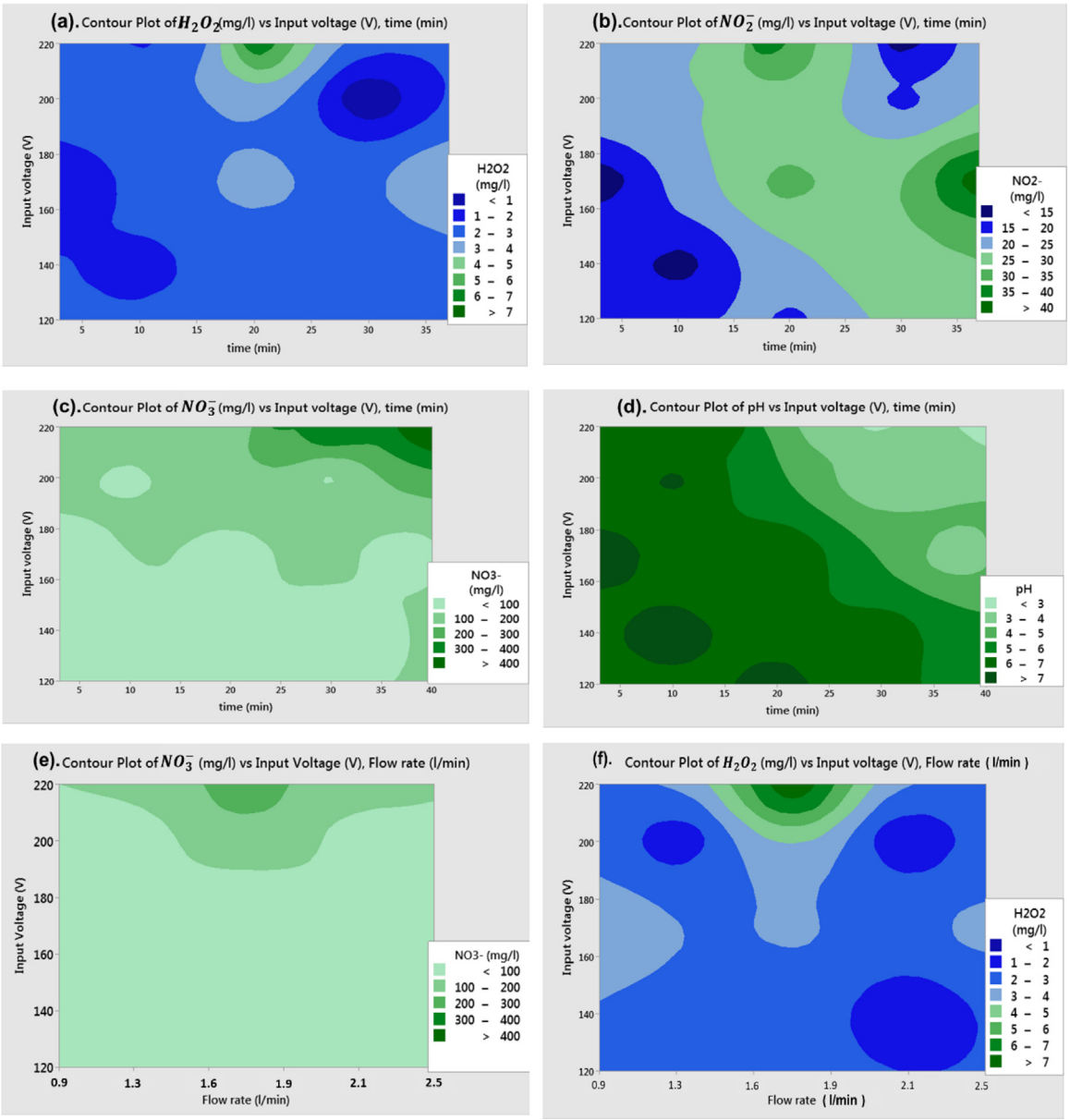

Fig. 5. H_2O_2, NO_2^- and NO_3^- concentrations and pH contour plots versus input voltage (V), treatment time (min) and water flow rate (l min^{-1}). ((a)–(d) contours depicted from data at water flow rate 1.75 and 2.1 l min^{-1}, and (e)–(f) at treatment time 20 min by the Minitab program).

Besides extensive analysis of the aqueous RONS formed in the PAW and its antibacterial effects in relation to the aqueous RONS, we examined the PAW effects on barley seeds germination as a representative agricultural application of PAW. Using normal control tap water and control water contaminated with *S. epidermidis* bacteria (bacterial solution, BS) and 4 repetitions, the germination percentage was 60% and 45%, respectively. It means that under our experimental conditions, the presence of *S. epidermidis* bacteria led to a decrease in seed germination. The effects of PAW treatment on the seed germination are presented in Fig. 6(d). In general, when the seeds were soaked by the PAW, the germination percentage increased by up to 20%, and in the highest case reached to 90%. The PAW prepared with maximum input voltage and after the optimum point of plasma treatment time ($\geq$20 min) increased germination percentage of barley seeds up to 80%. It should be noted that the PAW antibacterial properties lead to the prevention of reduced seed germination caused by contamination of wastewater with *S. epidermidis* bacteria.

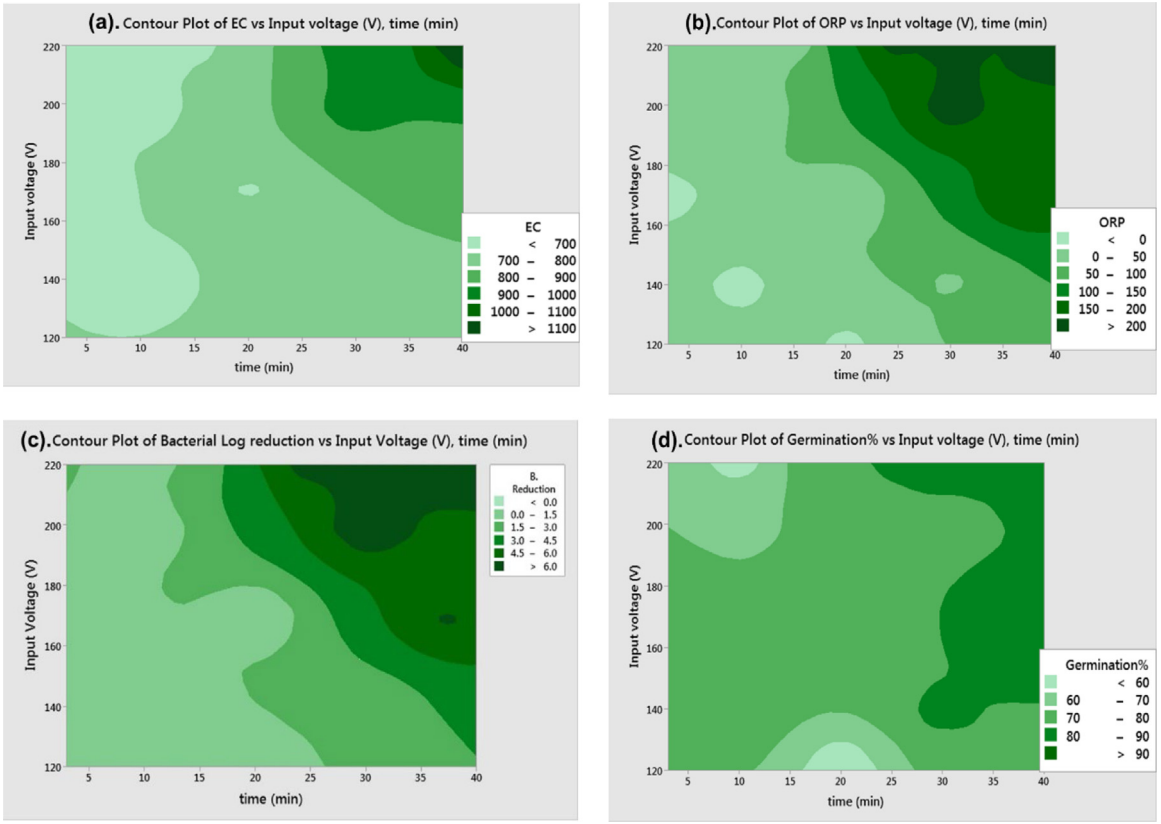

Fig. 6. ORP, EC, bacterial reduction and germination % contour plots versus main parameters (treatment time and input voltage) for 1750 ml min^{-1} water flow rate.

3.4. Optimum point in plasma treatment time and scale-up tests

3.4.1. RONS concentrations

The RSM investigation of the FDBD reactor operation showed that the optimum parametric area of the PAW treatment experiments appears on input voltage, water circulation flow rate and plasma treatment time around 220 V, 1750 ml min^{-1}, and 20 min, respectively. After finding the optimum parameter area, several experiments were repeated at the optimum flow rate and plasma input voltage to retrieve the exact behaviour of the FDBD reactor at different plasma treatment times for 1 l bacteria suspension (BS) treatment. We also repeated the experiments for 3 l BS to test a potential scale-up effect on the optimum point of plasma treatment time. Fig. 7 shows the concentrations of RONS obtained from 1 and 3 l BS plasma treatment with the FDBD reactor. To better show in this figure, the concentrations of nitrites and nitrates were multiplied by 0.1 and 0.01, respectively. The error bars in the experimental points represent the standard deviations from 4 repetitions data set. For longer treatment times than the optimum point (20 min) for 1 l BS, as shown in Fig. 7(a), the concentrations of nitrites and H_2O_2 were obviously decreased while NO_3^- concentrations were increased, which is due to the significant effects of the peroxynitrite mechanism and NO_2^- disproportionation after the optimum point.

The mechanism of nitrites and nitrates formation in water is the result of dissolution of nitrogen oxides and HNO_x formed in air plasma by reactions of dissociated N_2 and O_2 and OH radicals. It assumes that the difference in the concentrations of NO_2^- and NO_3^- measured in the plasma treated solutions is a result of subsequent post-discharge reactions leading to disproportionation of nitrites into nitrates occurring under acidic conditions, and peroxynitrite conversion to nitrates. Although the trend of the RONS concentration curves for plasma treatment of both 1 and 3 l BS using the FDBD reactor was the same, the 1 l plasma treatment time needs to be multiplied by 3 to obtain the same value of concentrations as in the case of 3 l BS plasma treatment. Therefore, the optimum plasma treatment time in the case of 3 l BS was determined at 60 min (Fig. 7(b)). We may expect that for even greater volumes of PAW generation using the same FDBD reactor, the optimum plasma treatment time (20 min for 1 l) for the same water flow rate 1750 ml min^{-1} can be found by linear scaling by the water volume.

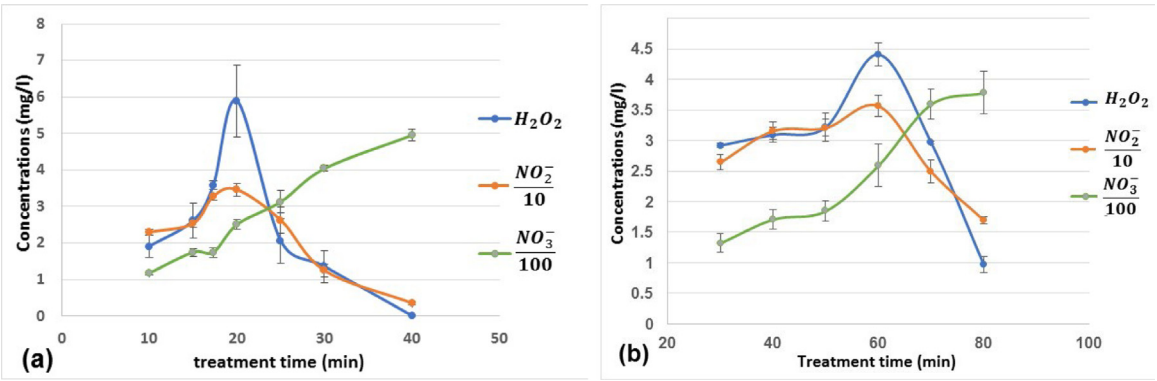

Fig. 7. Nitrite (NO_2^-), nitrate (NO_3^-) and hydrogen peroxide (H_2O_2) concentrations measured in (a) 1 l bacteria suspension, and (b) 3 l bacteria suspension, after plasma treatment using the FDBD reactor.

3.4.2. Bactericidal effect

Fig. 8 displays the bacteria log reduction, ORP, and pH values obtained from 1- and 3-litre BS plasma treatment in the FDBD reactor. The bacterial concentration was measured as 1.35×10^7 CFU ml^{-1} on average for the control group. As shown in Fig. 8(a) for both bacteria samples *E. coli* or *S. epidermidis*, the bacterial reduction results using the FDBD reactor are very similar. For 1 l BS, a significant bactericidal effect of PAW was achieved, with up to a 6-log reduction in *S. epidermidis* or *E. coli* population after 20 min of plasma treatment time. The standard deviation from four repetitions is indicated as the error bar in the bacterial results, but the error bars for the pH and ORP measurement were insignificant. This same trend was repeated in case of 3 l BS treatment after 60 min plasma treatment time (Fig. 8(b)). Apparently, the bactericidal effect of plasma treated solutions was accompanied by the significant changes in pH and ORP.

Our findings indicate that the overall bactericidal effect of air plasma discharge involves the synergistic effect of nitrites and peroxides under acidic conditions, which is consistent with our previous research (Soni et al., 2021; Machala et al., 2013). Lukes et al. explained that peroxynitrous acid/peroxynitrite ($ONOOH/ONOO^-$) is an unstable molecule that degrades into nitrate or in part, and more importantly, to $OH^\bullet$ and $NO_2^\bullet$ radicals. The antibacterial effect of peroxynitrous acid is primarily attributed to the production of these radicals, particularly $OH^\bullet$ radical. $OH^\bullet$ radical reacts with the phospholipids in the bacterial cell membrane, creating pores that lead to bacterial decay (Lukes et al., 2014; Xu et al., 2021).

Previous studies suggested that RONS are responsible for the inactivation of bacteria, particularly through the action of NO and $OH^\bullet$ radicals. These radicals can break down cell membranes and DNA structures, leading to cell death (Zhang et al., 2016). ROS, particularly H_2O_2 and $OH^\bullet$, can damage the structures of cell membranes and peptidoglycan bonds. PAW treatment can increase the leakage of cell membrane components such as extracellular DNA and intracellular proteins. The DNA damage can arrest the cell cycle, and increased oxidative stress is observed due to the presence of ROS, including superoxide ions (Dolezalova and Lukes, 2015). H_2O_2 is the main long-lived ROS in PAW, but short-lived ROS, such as OH, O, and $^1O_2$ and O_2^- also contribute indirectly to the increased ORP and oxidative stress to cell membranes and inner cell constituents. The effectiveness of PAW against bacteria is believed to be mainly due to the combined effects of low pH and high ORP that facilitate specific reactions, such as ONOOH formation (Eq. (3)) and its decay to OH radicals (Machala et al., 2018; Xu et al., 2020a).

RNS, such as NO radicals and their products, also contribute to the high ORP of PAW. RNS typically reduce the pH value of PAW and diffuse into bacterial cells, leading to bacterial inactivation. For example, the presence of NO in PAW can disperse biofilms and make the cells more susceptible to inactivation by antimicrobials (Zhou et al., 2020). Nitrites contribute to the formation of radicals by peroxynitrite formation (Eq. (3)) and decay, as mentioned previously. Furthermore, nitrite is antibacterial by itself, especially in acidic conditions, known as acidified nitrite (Traylor et al., 2011), which is in fact the undissociated form of nitrous acid HNO_2 at pH under its $pK_a = 3.4$ (Machala et al., 2018).

It should also be noted that if bacteria solutions are directly treated by plasma discharges, which is also our experimental condition presented here, the electric field of the discharge couples with the chemical PAW processes and enhances the antimicrobial effects. This was demonstrated in Mentheour and Machala (2022), where pulsed electric field synergized with RONS in PAW to enhance bacteria killing, and the effect was especially pronounced when significant concentrations of H_2O_2 and NO_2^- at acidic PAW conditions were present in the PAW and lead to ONOOH formation. We can hence assume that the electric field effect may contribute to antibacterial effect of RONS in the PAW also in the experiments presented here. However, despite extensive research worldwide, the specific detailed mechanisms underlying the antibacterial activity of PAW and direct plasma effects, and the individual contributions of specific reactive species are still not fully understood.

Furthermore, water treatment by the FDBD reactor raised the PAW temperature to approximately 45 °C during the optimum treatment time of 20 min per 1 litre (Fig. 3) and even higher for longer treatment times. To evaluate the

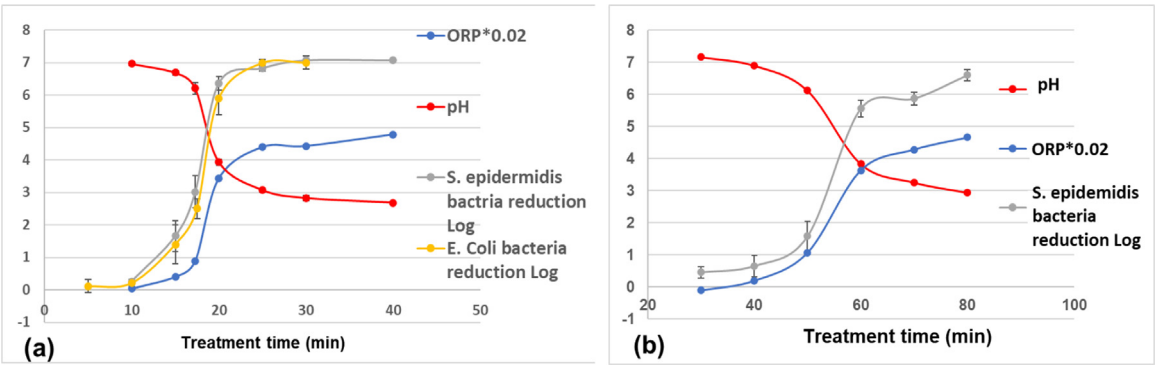

Fig. 8. Bacterial log reduction, Oxidation Reduction Potential (ORP) [mV], and pH measured in (a) 1 l S. epidermidis or E. coli bacterial solution, and (b) 3 l bacterial solution, after plasma treatment using the FDBD reactor.

bactericidal effects of the increased water temperature, we conducted a control experiment where we heated the BS while stirring using the same heating rate depicted in Fig. 3, but without plasma. The results showed that the heating process had a negligible impact on the antibacterial effect: heating 1 l of the BS to 45 °C and 55 °C within 20 and 30 min resulted in a reduction of the bacteria population by 0 and 0.3 log, respectively. However, increasing the temperature is recognized as a factor that supports the susceptibility of bacteria to plasma treatment and enhances their membrane permeabilization. In addition, elevated temperatures can enhance the kinetics of PAW chemistry, potentially limiting the bacteria's ability to repair damage resulting from RONS chemistry, so it cannot be neglected. However, up to optimum treatment time of 20 min per 1 l BS, the temperature effect was not responsible for the bacteria inactivation.

The results shown here (Figs. 7 and 8) confirmed that the optimum plasma treatment time for 1 l water in the FDBD reactor is 20 min, while the input voltage and water flow rate were kept at 220 V and 1.75 l min^{-1}, respectively. This optimum point of plasma treatment time indicates the minimum level of power consumption by the reactor per litre treated wastewater, which is needed to obtain maximum concentrations of nitrites and H_2O_2 in the PAW accompanied with a strong bactericidal effect. We also observed that the optimum time exhibits a linear scaling with the volume of wastewater treated in plasma. After this point (longer treatment times), the peroxynitrite mechanism quickly consumed H_2O_2 and NO_2^- and the bactericidal effect of PAW was saturated.

3.4.3. Seed germination improvement

In vitro cultivation of barley seeds was performed in Petri dishes using the plasma treated BS (representing contaminated water) by the FDBD reactor. The germination % of seeds cultivated in the PAW as a function of plasma treatment time evaluated after 4 days is depicted in Fig. 9 for both PAW generated from 1 and 3 l plasma treated BS. As shown in Fig. 9(a), the PAW produced for 1 l BS increased the germination % from 60 up to >80%. These effects are observed after 25 min plasma treatment time. The trend of germination % using 3 l plasma-treated BS in Fig. 9(b) matches the trend observed in Fig. 9(a), while the plasma treatment time is multiplied by 3. This is the same behaviour observed in the previous sections for the RONS concentrations variation at different plasma treatment times for 1 and 3 l BS. It indicates that improvement of the seed germination % is probably due to RONS accumulation in seeds in the early stages of imbibition, which was already reported for several plant species (Bailly, 2004; Schopfer, 2001). However, unlike saturation of bactericidal effect at 20 min (1 l BS), the germination percentage kept increasing with treatment time even after the optimum time point. This corresponds to NO_3^- production that also further increased with treatment time, which seems to be favourable for enhanced seed germination as a key nitrogen source for the seedlings.

Fig. 10 shows the germinated barley seeds soaked in the PAW (prepared from BS treatment) in comparison with the seeds soaked by control BS or normal tap water. The germination % of seeds cultivated in the BS and the tap water was observed up to 45% and 60%, respectively. The direct application of *S. epidermidis* bacteria-contaminated wastewater for seed germination poses multiple concerns, as high concentrations of *S. epidermidis* can adhere to seed surfaces, potentially impacting seed germination and seedling health. This bacterium's ability to form biofilms around the seeds may result in competition for nutrients, toxin production, tissue damage, and hindered seedling growth. Furthermore, if the contaminated wastewater contains plant pathogenic bacteria or fungi, the presence of *S. epidermidis* could facilitate the transmission of these pathogens to the seeds or seedlings (Fendri et al., 2013; Bharagava and Chandra, 2010).

The comparison of the germination % provided by the PAW with the control ones shows that the increase in germination % by the PAW samples was at least by 40% and in the best case it could reach up to 90%. The samples PAW 40, PAW 50, PAW 60, and PAW 70 in Fig. 10 were provided from 3 l plasma-treated BS by the FDBD reactor in 40, 50, 60, and 70 min plasma treatment times, respectively.

The positive effect of the PAW on seed germination can be caused by the effects of reactive oxygen species, such as H_2O_2, or reactive nitrogen species, such as NO_2^- and NO_3^-, which can stimulate germination and break seed dormancy.

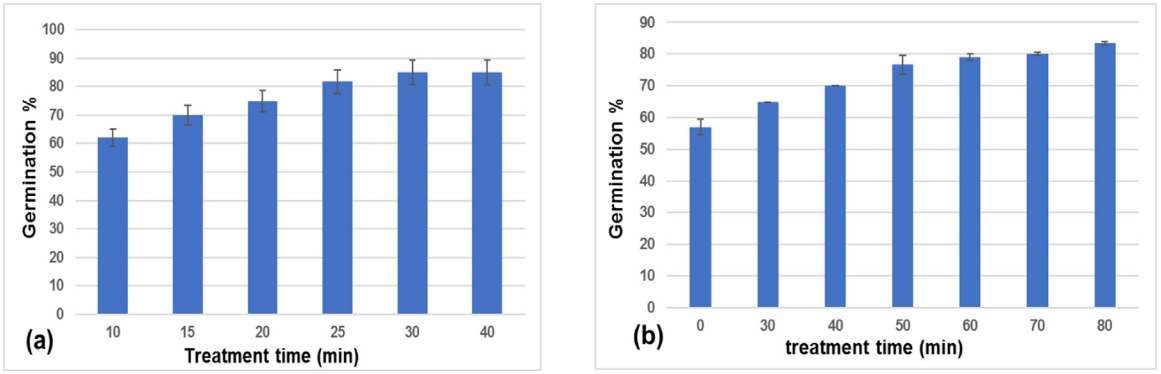

Fig. 9. Germination percentage of barley seeds that soaked with PAW produced in the FDBD reactor from (a) 1 l bacteria suspensions, and (b) 3 l bacteria suspensions.

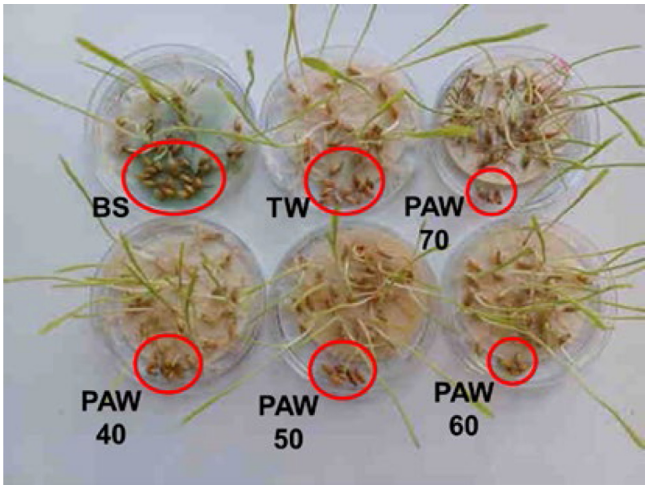

Fig. 10. The germination using the bacteria suspensions (BS), tap water (TW), and plasma-activated water (PAW) provided from BS plasma treatment at different plasma treatment times (min) for barley seeds soaking.

This effect of PAW treatment on the seed's germination enhancement confirms the previous reports in this area (Naumova et al., 2011; Fan et al., 2020). The use and transport of RONS in seeds are intricate processes. RONS, including H_2O_2, NO_2^-, NO_3^-, and ammonia (NH_4^+), produced in PAW, have been found to have beneficial effects on seed germination and seedling growth. The elevated levels of ROS in PAW can induce cracking of the seed coat, facilitating improved absorption of water and nutrients (Zhou et al., 2019). PAW also safeguards membrane lipids by boosting antioxidant enzyme activities and reducing the accumulation of malondialdehyde (MDA). H_2O_2 may stimulate respiration and metabolic activities by the production of O_2 during the catalase scavenging of H_2O_2. H_2O_2 in PAW activates genes associated with catalase (CAT) synthesis, thereby enhancing seed germination (Zhou et al., 2020). H_2O_2 can traverse plant cell membranes through diffusion and aquaporins, membrane proteins that aid in water transport (Bienert et al., 2006). It can also etch the seed's coat and facilitate the water diffusion, or it may oxidize germination inhibitors (Ogawa and Iwabuchi, 2001). Furthermore, seeds possess an enhanced capacity to detoxify H_2O_2 during the processes of imbibition and germination. Thus, the impact of PAW on seed germination depends on the response of seed metabolism to H_2O_2, encompassing antioxidant enzyme activity and cellular signalling (Kučerová et al., 2019). Additionally, NO_3^- can function as a signalling molecule, promoting the expression of genes involved in NO_3^- transport proteins and nitrate/nitrite reductase genes for NO_3^- assimilation (Polesskaya et al., 2004). Moreover, NO_2^- may also serve as a potential source of essential nitrogen (Kučerová et al., 2019). The diverse array of reactive species, with their varying concentrations, may contribute to the diverse outcomes observed in seed responses to PAW treatment, although the precise mechanisms remain only partially understood.

It should be noted that the electric field component may play a role in breaking seed dormancy and stimulating germination when seeds are directly exposed to the plasma. In our experiments the seeds were incubated only in PAW, without being directly exposed to the plasma. Thus, the increased germination effect can only be attributed to the RONS effect coupling with reduced bacterial population in the treated bacteria solutions. Although the exact mechanisms of PAW reactive species effects on seed physiology are not completely understood, the RONS in PAW may act as positive signal molecules to alleviate seed dormancy and stimulate seed germination by involving in abscisic acid/gibberellic acid signalling pathways or other mechanisms (Kučerová et al., 2019; Jeevan Kumar et al., 2015).

4. Conclusions

Energy efficient microbial decontamination process and sustainable agriculture both represent emerging global issues open to new technology solutions. Atmospheric-pressure non-thermal plasma represents a promising technology for wastewater treatment and recycling. In this study, we investigated chemical and bactericidal effects induced in regular tap water contaminated with *S. epidermidis* or *E. coli* bacteria representing microbial contamination by a new Fountain Dielectric Barrier Discharge (FDBD) reactor with liquid electrode. For both bacteria samples the bacterial reduction results using the FDBD reactor were very similar. The FDBD reactor was used to treat bulk quantity water (contaminated by bacteria) by non-thermal plasma. The air DBD plasma treatment led to the water acidification and increase of the oxidation–reduction potential and electrical conductivity, along with the production of Reactive Oxygen and Nitrogen Species (RONS): nitrites, nitrates, and hydrogen peroxide in the liquid. Using Response surface methodology, the optimum plasma treatment time as a main parameter of the reactor operation for producing maximum level of nitrites and peroxides in the liquid was determined, which was accompanied by strong bactericidal effect. After the optimum plasma treatment time, a sharp drop in pH was observed and nitrites were quickly oxidized to nitrates, while the bactericidal effect saturated. It was also observed that the optimal treatment time shows a linear correlation with the volume of wastewater processed by plasma. The plasma activated water, even produced from the bacteria-contaminated water, also stimulated the germination of seeds, as demonstrated on barley seeds in *in vitro* conditions. The germination percentage of seeds soaked in the PAW after the optimum plasma treatment time increased up to 85%, while the starting germination % using control tap water and the bacteria suspensions were 60% and 45%, respectively. The results demonstrate that the contaminated water treatment by the FDBD reactor not only shows a promising bactericidal effect (up to 7-log reduction), but also provides sufficient concentrations of RONS in the treated liquid to enhance the germination of barley seeds by more than 20%. It opens new plasma technology potential for a scalable treatment of microbially contaminated wastewater for its further reuse as a fertilizer solution in sustainable agriculture.

CRediT authorship contribution statement

Saeed Kooshki: Conceptualization, Methodology, Data curation, Formal analysis, Investigation, Project administration, Software, Validation, Visualization, Writing - original draft, Writing - review & editing. **Pankaj Pareek:** Data curation, Formal analysis, Writing – reviewing. **Robin Mentheour:** Data curation, Writing – reviewing. **Mário Janda:** Formal analysis, Data curation, Methodology. **Zdenko Machala:** Conceptualization, Funding acquisition, Supervision, Writing – review and editing.

Declaration of competing interest

The authors declare no financial interests/personal relationships which may be considered as potential competing interests.

Data availability

The data that has been used is confidential

Acknowledgements

This work was supported by Slovak Research and Development Agency APVV-17-0382 and APVV-22-0247 and Slovak Grant Agency VEGA 1/0596/22 and 1/0822/21, and by COST Action CA19110 "PlAgri" (supported by European Cooperation in Science and Technology).

References

Adamovich, I., et al., 2022. ET Jr, J. Trieschmann, S. Tsikata, MM Turner, IJ vd Walt, MCM vd Sanden, and T. v. Woedtke. J. Phys. D: Appl. Phys. 55, 373001. http://dx.doi.org/10.1088/1361-6463/ac5e1c.

Aka, R.J.N., Wu, S., Mohotti, D., Bashir, M.A., Nasir, A., 2022. Evaluation of a liquid-phase plasma discharge process for ammonia oxidation in wastewater: Process optimization and kinetic modeling. Water Res. 224, 119107. http://dx.doi.org/10.1016/j.watres.2022.119107.

Alberto, B., Lorenzo, R., 2019. Reassessing the projections of the world water development report. Npj Clean Water 2 (1), 15. http://dx.doi.org/10.1038/s41545-019-0039-9.

Ameta, S.C., Ameta, R., 2018. Advanced Oxidation Processes for Wastewater Treatment: Emerging Green Chemical Technology. Academic Press.

Anon, 2022. Drinking-water. [Online]. Available: https://www.who.int/news-room/fact-sheets/detail/drinking-water.

Bailly, C., 2004. Active oxygen species and antioxidants in seed biology. Seed Sci. Res. 14 (2), 93–107. http://dx.doi.org/10.1079/SSR2004159.

Barjasteh, A., Dehghani, Z., Lamichhane, P., Kaushik, N., Choi, E.H., Kaushik, N.K., 2021. Recent progress in applications of non-thermal plasma for water purification, bio-sterilization, and decontamination. Appl. Sci. 11 (8), 3372. http://dx.doi.org/10.3390/app11083372.

Bertaccini, A., et al., 2017. Plasma Activated Water To Enhance Plant Defenses, Presented At the Proceedings of the 23rd International Symposium on Plasma Chemistry.

Bharagava, R.N., Chandra, R., 2010. Effect of bacteria treated and untreated post-methanated distillery effluent (PMDE) on seed germination, seedling growth and amylase activity in Phaseolus mungo L. J. Hard Mater. 180 (1–3), 730–734. http://dx.doi.org/10.1016/j.jhazmat.2010.04.100.

Bienert, G., Schjoerring, J.K., Jahn, T.P., 2006. Membrane transport of hydrogen peroxide. Biochim. Biophys. Acta 1758, 994–1003. http://dx.doi.org/10.1016/j.bbamem.2006.02.015.

Bogaerts, A., et al., 2020. Plasma catalysis roadmap. J. Phys. D: Appl. Phy. 53 (44), 443001. http://dx.doi.org/10.1088/1361-6463/ab9048.

Canal, C., Labay, C., Ginebra, M., 2019. Important parameters in plasma jets for the production of RONS in liquids for plasma medicine: A brief review. Front. Chem. Sci. Eng. 13 (2), 238–252. http://dx.doi.org/10.1007/s11705-019-1801-8.

Dolezalova, E., Lukes, P., 2015. Membrane damage and active but nonculturable state in liquid cultures of escherichia coli treated with an atmospheric pressure plasma jet. Bioelectrochemistry 103, 7–14. http://dx.doi.org/10.1016/j.bioelechem.2014.08.018.

Ekanayake, U.M., et al., 2021. Utilization of plasma in water desalination and purification. Desalination 500, 114903. http://dx.doi.org/10.1016/j.desal.2020.114903.

Fan, L., Liu, X., Ma, Y., Xiang, Q., 2020. Effects of plasma-activated water treatment on seed germination and growth of mung bean sprouts. J. Taibah Univ. Sci. 14 (1), 823–830. http://dx.doi.org/10.1080/16583655.2020.1778326.

Fendri, I., Ben Saad, R., Khemakhem, B., Ben Halima, N., Gdoura, R., Abdelkafi, S., 2013. Effect of treated and untreated domestic wastewater on seed germination, seedling growth and amylase and lipase activities in Avena sativa L. J. Sci. Food Agric. 93 (7), 1568–1574. http://dx.doi.org/10.1002/jsfa.5923.

Gao, Y., Francis, K., Zhang, X., 2022a. Review on formation of cold plasma activated water (PAW) and the applications in food and agriculture. Food Res. Int. 111246. http://dx.doi.org/10.1016/j.foodres.2022.111246.

Gao, Y., Li, M., Sun, C., Zhang, X., 2022b. Microbubble-enhanced water activation by cold plasma. Chem. Eng. J. 446, 137318. http://dx.doi.org/10.1016/j.cej.2022.137318.

Ghavam, S., Vahdati, M., Wilson, I., Styring, P., 2021. Sustainable ammonia production processes. Front. Energy Res. 34, http://dx.doi.org/10.3389/fenrg.2021.580808.

Grabowski, L., Van Veldhuizen, E., Pemen, A., Rutgers, W., 2007. Breakdown of methylene blue and methyl orange by pulsed corona discharge. Plasma Sources. Sci. Technol. 16 (2), 226. http://dx.doi.org/10.1088/0963-0252/16/2/003.

Gururani, P., et al., 2021. Cold plasma technology: advanced and sustainable approach for wastewater treatment. Environ. Sci. Pollut. Res. 1–21. http://dx.doi.org/10.1007/s11356-021-16741-x.

Hadinoto, K., et al., 2023. Hybrid plasma discharges for energy-efficient production of plasma-activated water. Chem. Eng. J. 451, 138643. http://dx.doi.org/10.1016/j.cej.2022.138643.

Harley, J.C., Suchowerska, N., McKenzie, D.R., 2020. Cancer treatment with gas plasma and with gas plasma–activated liquid: Positives, potentials and problems of clinical translation. Biophys. Rev. 12 (4), 989–1006. http://dx.doi.org/10.1007/s12551-020-00743-z.

Herianto, S., et al., 2023. Chemical decontamination of foods using non-thermal plasma-activated water. Sci. Total Environ. 162235. http://dx.doi.org/10.1016/j.scitotenv.2023.162235.

Jeevan Kumar, S., Rajendra Prasad, S., Banerjee, R., Thammineni, C., 2015. Seed birth to death: dual functions of reactive oxygen species in seed physiology. Ann. Botany 116 (4), 663–668. http://dx.doi.org/10.1093/aob/mcv098.

Judée, F., Simon, S., Bailly, C., Dufour, T., 2018. Plasma-activation of tap water using DBD for agronomy applications: Identification and quantification of long lifetime chemical species and production/consumption mechanisms. Water Res. 133, 47–59. http://dx.doi.org/10.1016/j.watres.2017.12.035.

Kovačević, V.V., Dojčinović, B.P., Jović, M., Roglić, G.M., Obradović, B.M., Kuraica, M.M., 2017. Measurement of reactive species generated by dielectric barrier discharge in direct contact with water in different atmospheres. J. Phys. D: Appl. Phys. 50 (15), 155205. http://dx.doi.org/10.1088/1361-6463/aa5fde.

Kučerová, K., Henselová, M., Slováková, Ľ., Hensel, K., 2019. Effects of plasma activated water on wheat: Germination, growth parameters, photosynthetic pigments, soluble protein content, and antioxidant enzymes activity. Plasma Process. Polym. 6 (3), 1800131. http://dx.doi.org/10.1002/ppap.201800131.

Laux, C.O., 2002. Radiation and Nonequilibrium Collisional-Radiative Models. In: von Karman Institute Lecture Series, vol. 7, pp. 2002–2007.

Lukes, P., Dolezalova, E., Sisrova, I., Clupek, M., 2014. Aqueous-phase chemistry and bactericidal effects from an air discharge plasma in contact with water: evidence for the formation of peroxynitrite through a pseudo-second-order post-discharge reaction of H2O2 and HNO2. Plasma Sources. Sci. Technol. 23 (1), 015019. http://dx.doi.org/10.1088/0963-0252/23/1/015019.

MacFarlane, D.R., et al., 2020. A roadmap to the ammonia economy. Joule 4 (6), 1186–1205. http://dx.doi.org/10.1016/j.joule.2020.04.004.

Machala, Z., Tarabova, B., Hensel, K., Spetlikova, E., Sikurova, L., Lukes, P., 2013. Formation of ROS and RNS in water electro-s prayed through transient spark discharge in air and their bactericidal effects. Plasma Process. Polym. 10 (7), 649–659. http://dx.doi.org/10.1002/ppap.201200113.

Machala, Z., Tarabová, B., Sersenová, D., Janda, M., Hensel, K., 2018. Chemical and antibacterial effects of plasma activated water: Correlation with gaseous and aqueous reactive oxygen and nitrogen species, plasma sources and air flow conditions. J. Phys. D: Appl. Phys. 52 (3), 034002. http://dx.doi.org/10.1088/1361-6463/aae807.

Machala, Z., et al., 2007. Emission spectroscopy of atmospheric pressure plasmas for bio-medical and environmental applications. J. Mol. Spectrosc. 243 (2), 194–201. http://dx.doi.org/10.1016/j.jms.2007.03.001.

Magureanu, M., Mandache, N.B., Parvulescu, V.I., 2015. Degradation of pharmaceutical compounds in water by non-thermal plasma treatment. Water Res. 81, 124–136. http://dx.doi.org/10.1016/j.watres.2015.05.037.

Mentheour, R., Machala, Z., 2022. Coupled antibacterial effects of plasma-activated water and pulsed electric field. Front. Phys. 10, 895813. http://dx.doi.org/10.3389/fphy.2022.895813.

Milhan, N.V.M., Chiappim, W., da G. Sampaio, A., da C. Vegian, M.R., Pessoa, R.S., Koga-Ito, C.Y., 2022. Applications of plasma-activated water in dentistry: A review. Int. J. Mol. Sci. 23 (8), 4131. http://dx.doi.org/10.3390/ijms23084131.
Moorcroft, M.J., Davis, J., Compton, R.G., 2001. Detection and determination of nitrate and nitrite: a review. Talanta 54 (5), 785–803. http://dx.doi.org/10.1016/S0039-9140(01)00323-X.
Naumova, I., Maksimov, A., Khlyustova, A., 2011. Stimulation of the germinability of seeds and germ growth under treatment with plasma-activated water. Surf. Eng. Appl. Electrochem. 47, 263–265. http://dx.doi.org/10.3103/S1068375511030136.
Ndiffo Yemeli, G.B., Švubová, R., Kostolani, D., Kyzek, S., Machala, Z., 2021. The effect of water activated by nonthermal air plasma on the growth of farm plants: Case of maize and barley. Plasma Process. Polym. 18 (1), 2000205. http://dx.doi.org/10.1002/ppap.202000205.
Ogawa, K., Iwabuchi, M., 2001. A mechanism for promoting the germination of Zinnia elegans seeds by hydrogen peroxide. Plant Cell Physiol. 42 (3), 286–291. http://dx.doi.org/10.1093/pcp/pce032.
Patinglag, L., Melling, L.M., Whitehead, K.A., Sawtell, D., Iles, A., Shaw, K.J., 2021. Non-thermal plasma-based inactivation of bacteria in water using a microfluidic reactor. Water Res. 201, 117321. http://dx.doi.org/10.1016/j.watres.2021.117321.
Polesskaya, O., Kashirina, E., Alekhina, N., 2004. Changes in the activity of antioxidant enzymes in wheat leaves and roots as a function of nitrogen source and supply. Russian J. Plant Physiol. 51, 615–620. http://dx.doi.org/10.1023/B:RUPP.0000040746.66725.77.
Puač, N., Gherardi, M., Shiratani, M., 2018. Plasma agriculture: A rapidly emerging field. Plasma Process. Polym. 15 (2), 1700174. http://dx.doi.org/10.1002/ppap.201700174.
Qian, C., Dai, J., Tian, Y., Duan, Y., Li, Y., 2020. Efficient degradation of fipronil in water by microwave-induced argon plasma: mechanism and degradation pathways. Sci. Total Environ. 725, 138487. http://dx.doi.org/10.1016/j.scitotenv.2020.138487.
Rathore, V., Tiwari, B.S., Nema, S.K., 2022. Treatment of pea seeds with plasma activated water to enhance germination, plant growth, and plant composition. Plasma Chem. Plasma Process. 1–21. http://dx.doi.org/10.1007/s11090-021-10211-5.
Schopfer, P., 2001. Hydroxyl radical-induced cell-wall loosening in vitro and in vivo: implications for the control of elongation growth. Plant J. 28 (6), 679–688. http://dx.doi.org/10.1046/j.1365-313x.2001.01187.x.
Šerá, B., Scholtz, V., Jirešová, J., Khun, J., Julák, J., Šerý, M., 2021. Effects of non-thermal plasma treatment on seed germination and early growth of leguminous plants—A review. Plants 10 (8), 1616. http://dx.doi.org/10.3390/plants10081616.
Siciliano, V., Passerotto, R.A., Chiuchiarelli, M., Leanza, G.M., Ojetti, V., 2023. Difficult-to-treat pathogens: A review on the management of multidrug-resistant staphylococcus epidermidis. Life 13 (5), 1126. http://dx.doi.org/10.3390/life13051126.
Soni, A., Choi, J., Brightwell, G., 2021. Plasma-activated water (PAW) as a disinfection technology for bacterial inactivation with a focus on fruit and vegetables. Foods 10 (1), 166. http://dx.doi.org/10.3390/foods10010166.
Terebun, P., Kwiatkowski, M., Hensel, K., Kopacki, M., Pawłat, J., 2021. Influence of plasma activated water generated in a gliding arc discharge reactor on germination of beetroot and carrot seeds. Appl. Sci. 11 (13), 6164. http://dx.doi.org/10.3390/app11136164.
Thirumdas, R., et al., 2018. Plasma activated water (PAW): Chemistry, physico-chemical properties, applications in food and agriculture. Trends Food Sci. Technol. 77, 21–31. http://dx.doi.org/10.1016/j.tifs.2018.05.007.
Traylor, M.J., et al., 2011. Long-term antibacterial efficacy of air plasma-activated water. J. Phys. D: Appl. Phys. 44 (47), 472001. http://dx.doi.org/10.1088/0022-3727/44/47/472001.
Veronico, V., Favia, P., Fracassi, F., Gristina, R., Sardella, E., 2021. Validation of colorimetric assays for hydrogen peroxide, nitrate and nitrite ions in complex plasma-treated water solutions. Plasma Process. Polym. 18 (10), 2100062. http://dx.doi.org/10.1002/ppap.202100062.
Wardenier, N., et al., 2019. Removal of alachlor in water by non-thermal plasma: Reactive species and pathways in batch and continuous process. Water Res. 161, 549–559. http://dx.doi.org/10.1016/j.watres.2019.06.022.
Xu, H., Fang, C., Shao, C., Li, L., Huang, Q., 2022. Study of the synergistic effect of singlet oxygen with other plasma-generated ROS in fungi inactivation during water disinfection. Sci. Total Environ. 838, 156576. http://dx.doi.org/10.1016/j.scitotenv.2022.156576.
Xu, H., Ma, R., Zhu, Y., Du, M., Zhang, H., Jiao, Z., 2020a. A systematic study of the antimicrobial mechanisms of cold atmospheric-pressure plasma for water disinfection. Sci. Total Environ. 703, 134965. http://dx.doi.org/10.1016/j.scitotenv.2019.134965.
Xu, Y., Tian, Y., Ma, R., Liu, Q., Zhang, J., 2016. Effect of plasma activated water on the postharvest quality of button mushrooms, agaricus bisporus. Food Chem. 197, 436–444. http://dx.doi.org/10.1016/j.foodchem.2015.10.144.
Xu, D., et al., 2020b. Effects of plasma-activated water on skin wound healing in mice. Microorganisms 8 (7), 1091. http://dx.doi.org/10.3390/microorganisms8071091.
Xu, H., et al., 2021. Subcellular mechanism of microbial inactivation during water disinfection by cold atmospheric-pressure plasma. Water Res. 188, 116513. http://dx.doi.org/10.1016/j.watres.2020.116513.
Zhang, S., Rousseau, A., Dufour, T., 2017. Promoting lentil germination and stem growth by plasma activated tap water, demineralized water and liquid fertilizer. RSC Adv. 7 (50), 31244–31251. http://dx.doi.org/10.1111/1541-4337.12644.
Zhang, Q., et al., 2013. A study of oxidative stress induced by non-thermal plasma-activated water for bacterial damage. Appl. Phys. Lett. 102 (20), 203701. http://dx.doi.org/10.1063/1.4807133.
Zhang, Q., et al., 2016. Sterilization efficiency of a novel electrochemical disinfectant against staphylococcus aureus. Environ. Sci. Technol. 50 (6), 3184–3192. http://dx.doi.org/10.1021/acs.est.5b05108.
Zhou, R., Li, J., Zhou, R., Zhang, X., Yang, S., 2019. Atmospheric-pressure plasma treated water for seed germination and seedling growth of mung bean and its sterilization effect on mung bean sprouts. Innov. Food Sci. Emerg. Technol. 53, 36–44. http://dx.doi.org/10.1016/j.ifset.2018.08.006.
Zhou, R., et al., 2018. Cold atmospheric plasma activated water as a prospective disinfectant: The crucial role of peroxynitrite. Green Chem. 20 (23), 5276–5284. http://dx.doi.org/10.1039/C8GC02800A.
Zhou, R., et al., 2020. Plasma-activated water: Generation, origin of reactive species and biological applications. J. Phys. D: Appl. Phys. 53 (30), 303001. http://dx.doi.org/10.1088/1361-6463/ab81cf.